

NJC

Accepted Manuscript



This is an *Accepted Manuscript*, which has been through the Royal Society of Chemistry peer review process and has been accepted for publication.

Accepted Manuscripts are published online shortly after acceptance, before technical editing, formatting and proof reading. Using this free service, authors can make their results available to the community, in citable form, before we publish the edited article. We will replace this *Accepted Manuscript* with the edited and formatted *Advance Article* as soon as it is available.

You can find more information about *Accepted Manuscripts* in the [Information for Authors](#).

Please note that technical editing may introduce minor changes to the text and/or graphics, which may alter content. The journal's standard [Terms & Conditions](#) and the [Ethical guidelines](#) still apply. In no event shall the Royal Society of Chemistry be held responsible for any errors or omissions in this *Accepted Manuscript* or any consequences arising from the use of any information it contains.

Cite this: DOI: 10.1039/c0xx00000x

www.rsc.org/xxxxxx

FULL PAPERS

High Sensitive MRI Contrast Agent Enhanced Visualization of Tumor

Xiao-xia Song,^a Zhi-jun Liu,^a Xian-zhu Xu,^b Qun Tang^{*a}

Received (in XXX, XXX) Xth XXXXXXXXXX 20XX, Accepted Xth XXXXXXXXXX 20XX

DOI: 10.1039/b000000x

5 Compared with other medical imaging technique, MRI has an obvious disadvantage of low sensitivity, in other words, the injection dosage of probe (contrast agent) is very high. In this paper, we developed c(RGDyK)-conjugated KMnF₃ nanocubes as a tumor's targeting T₁ contrast agent. The short cycle peptide (c(RGDyK)) was conjugated with carboxylic terminated KMnF₃ nanoparticles via EDC coupling. The nanoparticles have appropriate hydrodynamic size and narrow distribution. Furthermore, it showed 10 highly in vitro bio-stability and biocompatibility. As the c(RGDyK)-conjugated nanoparticles were applied for in vivo MR imaging of tumor, it profoundly enhanced the image contrast as high as almost double. More important, the contrast agent's injection dosage is one to two orders lower than that of the commercial or reported one. The c(RGDyK) short peptide was proved to play targeting role, and c(RGDyK)-conjugated KMnF₃ nanoparticles have potential application for diagnosis of tumor.

15 Introduction

MRI, as a powerful medical imaging tool, has many advantages over other imaging modalities, such as limitless tissue depth, high spatial resolution, non-invasive and better contrast. MRI has its special probe, named as contrast agent (CA). CA 20 plays its role of shortening the relaxation time of excitable hydrogen and thus increasing the image's contrast between different tissues or abnormal organs. By assistance of CA MRI technique is capable of getting more precise anatomic structure even molecular events. However, the sensitivity for MRI contrast 25 agents is relatively low. Milli-molar (10⁻³–10⁻⁵ M) level of CAs (per metal atom basis) is generally required to obtain appreciable contrast in MR images, and the injection dosage is much higher than what other molecular imaging techniques needed (Positron emission tomography: 10⁻¹¹–10⁻¹² M, Single photon emission 30 computed tomography: 10⁻¹⁰–10⁻¹¹ M, optical imaging: 10⁻⁹–10⁻¹² M). High dosage might increase the risk of metal toxicity as well as nanotoxicity.¹ Targeting techniques are theoretically utilized to decrease the injection dosage by locally enriching agents in the region of interest. Bioconjugate techniques have been developed 35 for targeted diagnosis and therapy in the past decades.² Research toward the development of targeted MRI CAs has been ongoing in the past years, but the dosage of commercial or tested CAs is still quite high. Therefore it is urgently demanded to decrease the injection dosage of CA via targeting technique.

40 Angiogenesis is a critical process involving the formation of new blood vessels from pre-existing vessels, and solid tumors including breast cancer, ovarian cancer are considered to be angiogenesis-dependent since every increment in tumor cell population is preceded by an increase in new capillaries that 45 converge upon the tumors.³ Integrin $\alpha_v\beta_3$ is one of the most extensively studied biomarker of angiogenesis, as expression of

$\alpha_v\beta_3$ is dramatically augmented on the neovasculature of tumor but is not generally expressed on quiescent endothelial cells. The ability to noninvasively detect $\alpha_v\beta_3$ expression in living subjects 50 would allow a better characterization of tumors and help to identify tumor regions at early stage.⁴ A series of peptides containing arginine-glycine-aspartic acid (RGD) were designed as binding ligand for specifically combining with the tumor marker $\alpha_v\beta_3$, and moreover, these peptides have better cellular 55 uptake and are easy to synthesize via solid phase synthesis.^{5,6} RGD conjugated excitable NPs (Au, Fe₃O₄) have been developed for diagnosis of tumors.^{7,8,9}

Recently we developed KMnF₃ NP as a new type of biocompatible T₁ contrast agent with high relaxivity and proper 60 circulation time.^{10,11} Herein, we further present the RGD conjugated KMnF₃ NP as a high sensitive contrast agent for tumor targeting MR imaging. The PEG-COOH passivated NPs were initially synthesized by a thermal treatment with ligand exchange, and then the carboxylic terminated NPs was directly 65 conjugated with a short cycle peptide, cyclo (Arg-Gly-Asp-D-Phe-Lys) (c(RGDyK)), via the well-known EDC coupling process for bioconjugate. As administrated intravenously into the tumor-bearing mice, these c(RGDyK)-KMnF₃ NPs were dominantly delivered to the tumor vessels and residue for hours. 70 More surprisingly, even though the injection dosage is as low as 0.001mmol/kg the breast tumor can still be identified. Note that the tumor with the volume of smaller than 50 mm³ can easily be tracked by the clinical 3T MRI scanner.

Results and discussion

75 c(RGDyK)-conjugated KMnF₃ NPs were synthesized by three steps, In the first step, oleic acid passivated KMnF₃ NPs were synthesized using a previously described method,¹² and then PEG₅₀₀₀-COOH was exchanged with oleic acid and then coated

the NP on its surface. Finally EDC coupling reaction linked the amine group on the peptide with carboxylic group terminated PEG by formation of stable amide bond. This type of “exchange functional ligand/bioconjugated technique” is a classical protocol for functioning of nanoparticles for their bio-application. Our strategy was illustrated in Scheme 1.

As-synthesized NP was fully characterized before it was applied for in vivo targeted MR imaging. The perovskite structure of the KMnF_3 NPs was confirmed by X-ray diffraction (XRD) analysis (not shown here). Figure 1a shows the transmission electron microscopy (TEM) image of the cubic-shaped KMnF_3 NPs with the uniform width around 20 nm. Note that the morphology of KMnF_3 NPs is determined by the synthetic protocols.^{10,11} HRTEM image of an individual nanoparticle (figure 1b) displayed a clearly resolved lattice fringe of (110) planes ($d_{110} = 0.294$ nm), the corresponding electron diffraction pattern demonstrated its well crystallization, as inserted images showed. The surface coating was confirmed by Fourier transform infrared spectroscopy (FTIR). In the FTIR spectrum, there was a characteristic peak for the amide bond because the activated carboxylate during EDC coupling reacts with an amine to give a stable amide linkage. These characteristic peaks were revealed at $3,423\text{ cm}^{-1}$ (N–H stretch), $1,633\text{ cm}^{-1}$ (N–H bend), and $1,061\text{ cm}^{-1}$ (C = N stretch). Two peaks ($1,560\text{ cm}^{-1}$, $1,456\text{ cm}^{-1}$) are attributed from aromatic framework stretching vibration, and $1,262\text{ cm}^{-1}$, $1,011\text{ cm}^{-1}$ peaks are due to C–O–C bond's antisymmetric and symmetric stretching vibration, and both are attributed to PEG moiety. Therefore they are undetectable in the FT-IR spectrum of pure c(RGDyK) peptide (Fig. S1). Some peaks were assigned in figure 1c, and the spectrum is similar to the reported one.¹³ Note that C=O stretching band is difficult to define due to its overlapping with N-H bending band. These data strongly demonstrate that the desired c(RGDyK)- KMnF_3 NPs were successfully synthesized. Although we have not estimated the exact number of RGD peptide per particle. We have evaluated the conjugation efficiency by clarifying mass distribution to conjugated state/free state, and free peptide in the side products or supernatant against dialysis is almost undetectable by mass spectra measurements. The NPs are stable in physiological condition since the hydrodynamic size of the NPs is around 150 nm with narrow distribution, as monitored with dynamic light scattering in figure 1d. Furthermore, size and its distribution of the NPs changed very slightly after 24 hours (not shown here), and agglomeration was not observed in several weeks by naked eyes. These particles are expected to have high bio-stability in the body.

The c(RGDyK)- KMnF_3 NPs displayed high T_1 relaxivity, as shown in Fig. 2a. The specific relaxivity, defined as the relaxation rate per mM of Mn ions, quantitatively reflects the efficiency of contrast enhancement by the magnetic nanoparticles as MRI contrast agents. The calculated r_1 value of the nanoparticulate contrast agent was $22.58\text{ mM}^{-1}\cdot\text{s}^{-1}$ under 3 T magnetic field, which is comparable with the reported PEGylated KMnF_3 nanoparticles, and the relatively large r_1 value is determined by the surface state of low valence stabilized Mn ions.^{10,11} To preliminarily evaluate the possible toxicity, the kidney cell's

viability against the NPs was carried out with the typical MTT protocol. As shown in Fig. 2b, the nanoparticulate contrast agent did not show obvious cytotoxicity at a test concentration of up to 0.01 mg/ml, which is lower than the injected one. Therefore, the nanoparticulate CA has very low cytotoxicity.

In-vivo target MRI through administrated c(RGDyK) conjugated KMnF_3 NPs was examined. Mice bearing breast cancer through implanting MDA-MB-231 cells under skin through the standard protocol. Angiogenesis of the tumor was proved by cluster of differentiation 31 (CD31) immunohistochemistry staining. It helps to evaluate the degree of tumor angiogenesis. The staining microscopy image indicates the presence of blood vessels in the tumor tissue, therefore a certain degree of tumor angiogenesis, as the arrow points in figure 3a. It is reasonable that as the tumor size is larger than 2 mm angiogenesis will occur and it is expected that integrin $\alpha_v\beta_3$ will be expressed. Very low dosage of nanoparticulate contrast agent (0.001 mmol/kg) was intravenously injected into breast cancer-bearing mice. After two hours, tumor was excised and stained for microscopy analysis. Electron microscopy of the tumor slice demonstrated the presence of nanoparticles in the tumor tissue (Fig. 3b). It demonstrated that c(RGDyK) conjugated KMnF_3 NPs have high affinity with the tumor via the specific peptide-integrin interaction.

MR images were recorded before injection, right after injection and two hours after injection of the same dosage of the CA. As shown in figure 4, the peptide conjugated NPs obviously enhanced the image contrast of the tumor with a volume of less than 50 mm^3 , even two hours after administration the tumor still can be discriminated from the surrounding tissue, the tumor contrast ratio for the three time points is 1:1.8:1.6. To confirm the bio-recognition between the peptide and target integrin $\alpha_v\beta_3$, free c(RGDyK) peptide was pre-injected in the control mice and maintained for two hours before administration, it can be found that right after injection, the tumor can be identified although the signal of tumor to the background is not strong as that in the absence of peptide pre-administration. Two hours later, the enhanced tumor signal almost disappeared, and the corresponding contrast ratio is 1:1.2:1.1. It is plausible that due to the integrin $\alpha_v\beta_3$ in the tumor cell has dominantly integrated with pre-injected peptide, so conjugation of free peptide with the integrin makes the target saturated and the lateral feeding peptide with the NPs has no chance to specifically interact with $\alpha_v\beta_3$. Although we still found the weak enhancement signal, this contrast enhancement mainly contributed from passive target delivery and imaging. As the incomplete tumor vasculature causes leaky vessels with enlarged gap junctions, nanoparticles, easily access the tumor interstitium. NPs have longer retention time in tumor than normal tissues because tumors lack a well-defined lymphatic system. These features provide an enhanced permeability and retention (EPR) effect, which constitutes an important mechanism for the passive targeting and selective accumulation of nanoparticles in the tumor interstitium.^{14,15} However, due to lack of the specific interaction, the retention time for contrast agent in the tumor interstitium will be shorter since it was soon metabolized and excreted out from the tumor, as displayed in figure 4. To be mentioned, solid tumor experiences initial state with the size of

millimeter before its rapid proliferation and deadly metastasis. However, clinically it is not easy to define a tumor with the size below 5 mm, even 1 cm. Herein, we can clearly found the tumor with the width of around 4 mm with the volume less than 50 mm³. Therefore, the nanoparticulate contrast agent might be useful for early detection of tumor.

c(RGDyK) conjugated KMnF₃ NPs have greatly enhanced MRI contrast of mammary tumor in the early stage, more importantly, the dosage is unprecedentedly as low as 0.001 mmol/kg, which is much lower than the commercial CAs or reported ones, as listed in table.1. Considering the content of metal Mn in animals' organism ranged from 0.0019 to 0.055 mmol/kg, it can be anticipated that this new type of MRI contrast agent might be applicable as a biocompatible contrast agent for the clinic. Even low dosage of the nanoparticulate CA was administered, MR images still showed enough high contrast to identify tumor from surrounding tissues. Three reasons are attributed to the high sensitivity. Firstly, compared to the small molecular contrast agent, nanoparticles have longer circulation time (minutes vs hours),¹⁷ and the contrast agent has more chance to go through the tumor tissue through cardiovascular system via the EPR effect. This passive target delivery system is also helpful to detect tumor, as we demonstrated in the control group. However, due to lack of strong interaction, they have less residue time within tumor and metabolized through kidney, liver or spleen very soon. Our targeting strategy is based on specific bio-recognition between RGD peptide on the surface of KMnF₃ NPs and integrin $\alpha v \beta 3$, a type of cell surface receptor, expressed on tumoral endothelial cells. Cyclic RGD peptide conjugated NPs have high affinity with on the surface of tumoral endothelial cell and concentrated within the neovasculature of the tumor. Secondly, the small nanoparticles capping with PEG tend to avoid nonspecific adsorption of serum proteins, and longer circulation time can be acquired.^{18,19} The plasma protein adsorption to NPs is ease to opsonization, a process that involves surface deposition of blood opsonic factors (such as fibronectin) for enhanced recognition by macrophages,²⁰ the as-synthesized c(RGDyK)-KMnF₃ NPs have small size, more importantly, PEG chain might be helpful to avoid the clearance by the mononuclear phagocyte system(MPS). Finally, the c(RGDyK)-KMnF₃ NPs have higher relaxivity than other commercial Gd agents as well as other Mn-based nanoparticulate contrast agents, as we explained in reference 10. Therefore, as shown in table 1, the injection dosage of MRI CA decreased to the unprecedentedly low value (0.001 mmol/kg). Note that "low sensitivity" does not correlate with the intrinsic detection limitation of MRI. Every type of imaging modality has its detecting inferior limit of corresponding probes. Although MRI has the lower detected limitation of CAs, very low dosage of the nanoparticulate contrast agent can still be concentrated inside the tumor through active target delivery, and it profoundly enhance the visualization of tumor, even small lesions.

Conclusions

In summary, c(RGDyK) conjugated KMnF₃ NPs was explored as a new type of tumor-target T₁ nanoparticulate contrast agent. The contrast agent was specifically delivered to the small tumor, and

made it easier to be visualized by MRI even at very low dosage. It is anticipated that the c(RGDyK)-KMnF₃ NPs might pave its way to clinical molecular imaging. Furthermore, due to the small size of the tumor, the contrast agent is expected for diagnosis of tumor in the early stage.

Materials and Methods

Synthesis of 25 nm carboxylic terminated PEGylation KMnF₃ NPs. MnCl₂·4H₂O (99+%), potassium oleate (99+%), NaOH (98+%), KF (99+%), 1-octadecene (90%), oleic acid (90%), and oleylamine (70%) were purchased from Sigma-Aldrich, PEG-COOH (MW:~5000 Da) were ordered from Shanghai Seebio Biotech, Inc. All the chemicals were used as starting materials without further purification. In a typical procedure to the synthesis of cubic KMnF₃ nanocrystals, manganese oleate (197.7 mg), prepared according to reference 21, was added to a flask containing a mixture of oleylamine (1 mL), oleic acid (1 mL), and 1-octadecene (8 mL) under vigorous stirring at room temperature. The resulting mixture was then heated at 150°C until the solution turned from colorless to yellowish. After cooling to room temperature, a methanolic solution (2 mL) of KF (1.2 mmol) was injected into the flask. The mixture was stirred at 65°C for 30 min and then purged by nitrogen at 105 °C for 30 min. Subsequently, the temperature was raised to 290°C and maintained for 60 min under nitrogen atmosphere. Finally, the reaction was cooled to room temperature. The as-prepared nanocrystals were collected by centrifugation, washed with ethanol and methanol three times. Surface grafting with carboxylic terminated PEG was done by co-heating KMnF₃ NPs with PEG(5000)-COOH powder in ethanol with molar ratio of 1:10 at 70°C for 12 hours, after cooling down, the sample was washed with ethanol and naturally dried.

Conjugation of c(RGDyK) peptide to KMnF₃ NPs. 1-ethyl-3-(3-dimethylaminopropyl)-carbodiimide (EDC, 34 mg), N-hydroxysulfosuccinimide (Sulfo-NHS, 34 mg), and 1 mg c(RGDyK) were added to 4 mL of the carboxylic terminated PEGylation KMnF₃ NPs (15 mg) solution and reacted at 4 °C for 12 hours. After the reaction, side products were removed by centrifugation at 15,000 rpm for 30 minutes and subsequently dialysis against pure water for three times at 4 degree. The nanoparticulate contrast agent powder showed slightly grey and colorless NPs solution showed undetectable degradation or aggregation over weeks. TEM images were taken on JEM 2100 (120kV). FT-IR spectrometer (Mattson Instruments, Inc., Galaxy 7020A) was used to prove the surface conjugation of the KMnF₃ nanoparticle. We slightly modified the traditional KBr pellet pressing method since light baking might de-active peptide, instead we put the sample in a dry environment. Note that the metal Mn²⁺ concentration in the NP solution for relaxivity measurement, cytotoxicity, and in-vivo MRI was determined by inductively coupled plasma atomic emission spectrometer (ICP-AES) (ICP-AES OPTIMA 5300DV, PE company). DLS spectrum of the nanoparticle was measured by DynaPro NanoStar (Wyatt) at room temperature.

Relaxivity measurement. The T₁-weighted MR images were obtained using a 3 T clinical MRI scanner (Siemens). Dilutions of c(RGDyK)-conjugated KMnF₃ (2, 1, 0.5, 0.02mM of Mn ions) in

deionized water were loaded into a capsule for T1-weighted MR imaging and T1-weighted contrast enhancement. The r_1 relaxivity values were obtained from the slopes of the $R(1/T)$ versus Mn concentration plots.

Cytotoxicity measurement. Cell viability was determined in kidney cells maintained in grow media (RPMI 1640 and Leibovitz's L-15 media with L-glutamin, 1% antibiotic-antimycotic, 10% fetal bovine serum) at 37 °C in a humidified atmosphere of 5% of CO₂. Cytotoxicity of NPs was evaluated by measuring the inhibition of cell growth using the MTT assay. Briefly, cells were plated at a density of 5×10^3 cells/ml in 96-well plates and treated with the above compounds for 24 h. After treatment, the cells were washed and incubated for an additional 3 h. Cell viabilities were calculated as the ratio of the number of cells treated to the number of non-treated control cells. Cell viability graphs were plotted against Mn²⁺ concentration of the NPs solution.

Mammary Tumor-bearing Mice and In Vivo MRI Studies.

All the animal treatment was conducted in conformity with institutional guidelines for the care and use of laboratory animals in Nanchang University. BALB/c female nude mice with 5-6 weeks age and weighted around 20 g were purchased from shanghai Slac Company. The mice were grown in the standard SF animal room. MDA-MB-231 cell were cultured in 1640 culture solution (invitrogen company) containing 10%BSA, 100U penicillin and 100U streptomycin at the temperature of 37°C and 5% CO₂. Cell in PBS solution (0.1 ml, 1×10^7) were injected subcutaneously into the dorsal skin of the mice, and the mice was culture for ten days, and the width of the cell measured by MRI is less than 4 mm with calculated volume of around 50 mm³. MR imaging was performed using a Siemens 3.0 Tesla whole body clinical MR scanner. MR images were acquired using a spin-echo T1-weighted MRI sequence (TR/TE = 600/14 ms, slice thickness = 0.7 mm, FOV = 50 * 50, matrix size = 512 * 512) and read the brightness ratio to evaluate. Mice were anesthetized and then c(RGDyK)-KMnF₃ NPs solution were injected intravenously with the Mn dosage of 0.001 mmol/kg. In case of the control group, pure c(RGDyK) (dosage: 10 mg/kg) was pre-injected into tail vein and maintained for one hours before the same dosage of c(RGDyK)-KMnF₃ NPs solution was administrated.

Immunohistochemical staining and electron microscopy of tumor slice. Tumor was excised into halves two hours after injection, and half part was fixed in 4% formalin and paraffin embedded for CD31 immunohistochemical staining. The staining protocol follows the standard HRP-DAB color-developing method. The whole tumor area was evaluated under light microscopy. Another half tissue were placed in formalin-glutaraldehyde for electron microscopy (EM) with subsequent process (fixing by osmic acid, dehydration, embed, solidification, section (70 nm), staining with uranyl acetate and lead citrate). All the process follow the standard protocol describe in the book "Electron Microscopy, Principles and Techniques for Biologists", written by John J. Bozzola and Lonnie D. Russell, published by Jones and Bartlett, 1992.

Acknowledgements

This work is financially supported by the National Natural

Science Foundation of China (21361018). The authors appreciate Xiao-zeng You (Nanjing University), Jian-qi Li (Shanghai Key Lab of Magnetic Resonance) for helpful discussion and in-vivo MRI operation, and also thank Dr. Bin-bing Tang for TEM technical support.

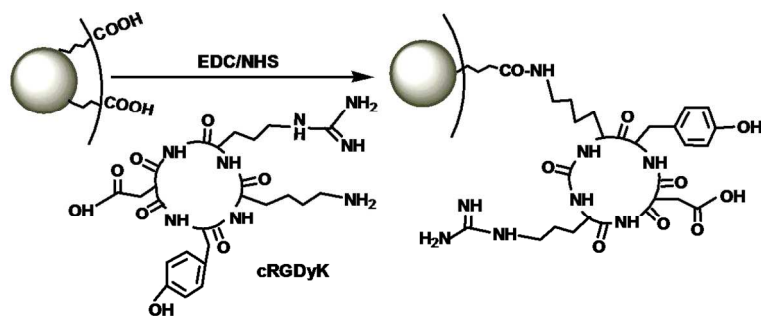
Notes and references

^a Institute for Advanced Study, Nanchang University, Nanchang, China.

^b College of Life Science, Jiangxi Normal University, Nanchang, China.

† Electronic Supplementary Information (ESI) available: [FT-IR spectrym of pure c(RGDyK) peptide]

1. R. Weissleder and J. M. Pittet, *Nature* 2008, **452**, 580–589.
2. E. I. Zenkevich, S. V. Gaponenko, E. I. Sagun, and C. von Borczyskowski, *Rev. Nanosci. Nanotechnol.* 2013, **2**, 184-207.
3. J. Folkman, *N. Engl. J. Med.* 1971, **285**, 1182-1186.
4. D. A. Sipkins, D. A. Cheresch, M. R. Kazemi, L. M. Nevin, M. D. Bednarski and K. C. Li, *Nat. Med.* 1998, **4**, 623-6.
5. F. Danhier, A. L. Breton and V. Préat, *Mol. Pharmaceutics* 2012, **9**, 2961-2973.
6. S. Zitzmann, V. Ehemann and M. Schwab, *Cancer Res.* 2002, **62**, 5139-5143.
7. J. Xie, K. Chen, H. Y. Lee, C. Xu, A. R. Hsu, S. Peng, X. Chen and S. Sun, *J. Am. Chem. Soc.* 2008, **130**, 7542-7543.
8. D. Arosio, L. Manzoni, E. M. V. Araldi and C. Scolastico, *Bioconjugate Chem.* 2011, **22**, 664–672.
9. Y. Liu, Y. Yang and C. Zhang, *International Journal of Nanomedicine* 2013, **8**, 1083–1093.
10. Z. Liu, X. Song and Q. Tang, *Nanoscale* 2013, **5**, 5073–5079.
11. Z. Liu, X. Song, X. Xu and Q. Tang, *Nanotechnology* 2014, **25**, 155101-155108.
12. J. Wang, F. Wang, C. Wang, Z. Liu, X. Liu, *Angew Chem Int Ed.* 2011, **50**, 10369–10372.
13. J. Choi, J. Yang, J. Park, E. Kim, J. S. Suh, Y. M. Huh and S. Haam, *Adv. Funct. Mater.* 2011, **21**, 1082–1088.
14. H. Maeda, J. Wu, T. Sawa, Y. Matsumura and K. Hori, *J. Control Release*, 2000, **65**, 271-284.
15. I. Brigger, C. Dubernet and P. Couvreur, *Adv Drug Deliv Rev.* 2002, **54**, 631-651.
16. B. Romberg and G. Storm, *Pharm Res.* 2008, **25**, 55-71.
17. M. A. Dobrovolskaia and S. E. McNeil, *Nat. Nanotech.* 2007, **2**, 469-478.
18. S. E. McNeil, *Wiley Interdiscip Rev Nanomed Nanobiotechno* 2009, **1**, 264-271.
19. H. S. Choi, L. W. P. Misra, E. Tanaka, J. P. Zimmer, B. I. Ipe, M. G. Bawendi and J. V. Frangioni, *Nat. Biotech* 2007, **25**, 1165-1170.
20. H. B. Na, J. H. Lee, K. An, Y. I. Park, I. S. Lee, D.-H. Nam, S. T. Kim, S.-H. Kim, S.-W. Kim, K.-H. Lim, K.-S. Kim, S.-O. Kim and T. Hyeon, *Angew. Chem. Int. Ed.*, 2007, **46**, 5397.
21. J. Park, K. An, Y. H. J. G. Park, H. J. Noh, J. Y. Kim, J. H. Park, N. M. Hwang and T. Hyeon, *Nat. Mater.* 2004, **3**, 891



Scheme 1. Schematic illustration of the EDC coupling c(RGDyK) to the carboxylic exposed KMnF₃ NP.

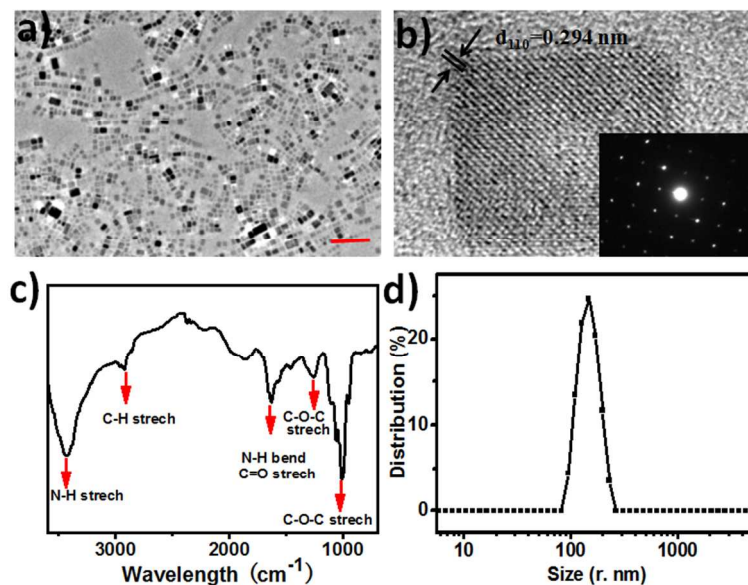


Fig. 1 a) Low-resolution TEM image of the as-synthesized cube-shaped c(RGDyK)-KMnF₃ NPs. Scale bar: 100 nm. b) High-magnification TEM image of a single cubic NP inserted with the corresponding electron diffraction pattern. c) FT-IR spectrum of the c(RGDyK)-KMnF₃ NPs demonstrated that cyclic RGD peptide was anchored on the surface of the NPs. d) hydrated diameter distribution curve of the c(RGDyK)-KMnF₃ NPs in physiological condition.

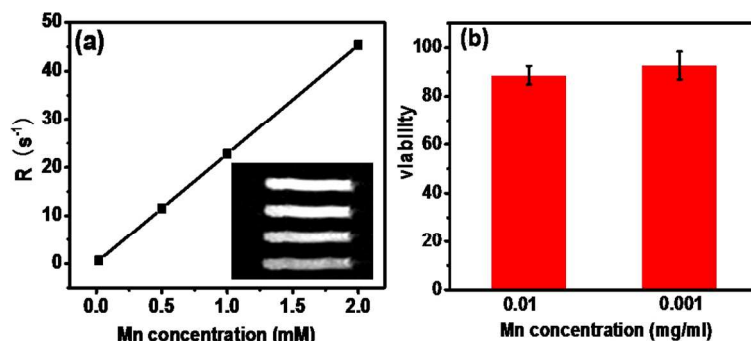


Fig. 2 a) Plots of R_1 relaxations of the c(RGDyK)-conjugated KMnF₃ nanoparticles solutions as a function of Mn concentration produces r_1 value (22.58 mM⁻¹s⁻¹) and corresponding T_1 -weighted mapping images (insert). b) Kidney cell viability is around 90% as it was incubated with the c(RGDyK)-conjugated KMnF₃ nanoparticles solutions, the solutions contain the metal solution from 0.01 mg/ml to 0.001 mg/ml.

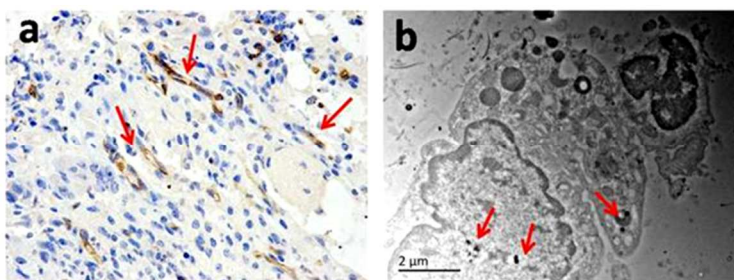


Fig. 3 (a) Immunohistochemistry staining microscopy of the tumor slice excised from the mice before administration confirm the existence of angiogenesis in the tumor, as the red arrow indicated. (b) Electron microscopy of the tumor slice excised after administrated with c(RGDyK)-KMnF₃ NPs indexed as the red arrow pointed.

5

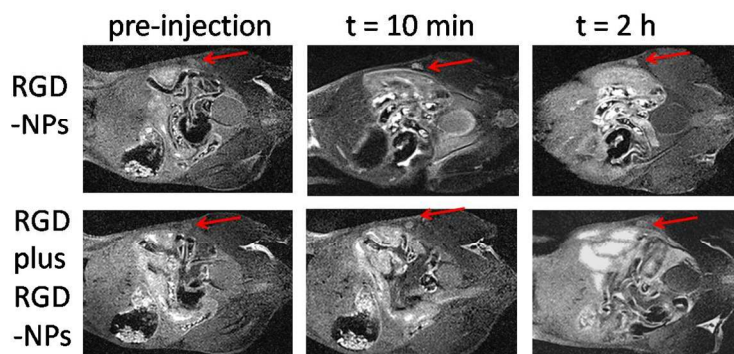


Fig. 4 Time-resolved MRI of the tumor-bearing mice after administration of c(RGDyK)-KMnF₃ NPs (above) and the control group with RGD peptide pre-injection (below). The small tumor as the red arrows point can be clearly distinguished under the skin at 10 min after intravenous injection, and keep visibility after 2 hours. In comparison, RGD saturated tumor is less clarified after administration of c(RGDyK)-KMnF₃ NPs.

10

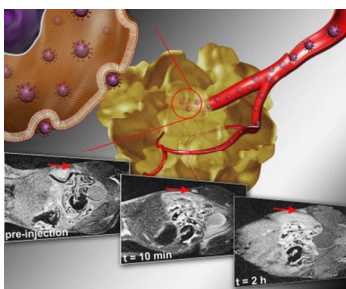
MRI Contrast Agent	Gd-DTPA (Magnevist)	Gadodiamide (Omniscan)	Gadofosveset (Vasovist)	Fe ₃ O ₄ (Feridex)	Mn-DPDP (Mangafodipir)	RGD-coated Fe ₃ O ₄ 6	Herceptine Coated MnO(18)	RGD-coated KMnF ₃
Injection dose	0.1	0.1	0.03	0.01	0.05	0.065	0.37	0.001
Metal (mmol kg)								
Application	human	human	human	human	human	mice	mice	mice
CA type	T ₁	T ₁	T ₁	T ₂	T ₁	T ₂	T ₁	T ₁

Table. 1 Comparison of the commercial or reported CAs with c(RGDyK) conjugated KMnF₃, and the latter has the lowest dosage.

15

20

Graphic Table of Contents



We developed c(RGDyK)-conjugated KMnF_3 NPs as a high sensitive T_1 contrast agent with tumor target imaging, and achieved optimal tumor to background ratio under injection dosage of 10^{-3} mmol/kg.